

LETTER TO THE EDITOR



Cryo-EM structure of the type III-E CRISPR-Cas effector gRAMP in complex with TPR-CHAT

© CEMCS, CAS 2022

Cell Research (2022) 32:1128–1131; <https://doi.org/10.1038/s41422-022-00738-3>

Dear Editor,

Prokaryotes and viruses have been engaged in an evolutionary struggle for billions of years.¹ Bacteria and archaea employ clustered regularly interspaced short palindromic repeats (CRISPR)-CRISPR-associated (Cas) adaptive immune systems to protect against viral infection.² The CRISPR-Cas locus consists of two parts: CRISPR and Cas genes. According to the latest phylogenetic classification, the CRISPR-Cas system can be divided into two classes, which can be further subdivided into six types.³ Class 1 CRISPR-Cas systems are characterized by a multiprotein effector, and consist of type I, III, and IV CRISPR-Cas systems. Class 2 CRISPR-Cas systems feature a single nuclease protein, and consist of type II, V, and VI CRISPR-Cas systems. The type II Cas9 and type V Cas12 systems have been engineered as genome editing tools, and they have been successfully applied in a broad range of organisms.^{4,5} Compared to Cas9, the type VI Cas13 system exhibits RNA-guided RNase activity and the property of nonspecific cutting.⁶ Recently, a new subtype of CRISPR-Cas, type III-E,³ has been identified and named gRAMP⁷ or Cas7-11.⁸ Unlike the traditional effectors of the type III CRISPR-Cas system, gRAMP is a single effector protein with four Cas7 proteins and one Cas11 protein fused together. Given its unique architecture and specific cleavage activity, gRAMP is expected to be engineered as a powerful RNA editing tool.⁸ Interestingly, a gene encoding the caspase-like peptidase TPR-CHAT often co-occurs with gRAMP gene clusters.³ TPR-CHAT interacts directly with gRAMP,⁷ indicating a functional relationship between the CRISPR-Cas system and caspase peptidase. However, the exact mechanism of the recognition and cleavage of target ssRNA by gRAMP from *Candidatus "Scalindua brodae"* (*Sb*-gRAMP),⁷ as well as the molecular architecture of the CRISPR-guided caspase complex, remain unclear.

In this study, we determined the cryo-electron microscopy (cryo-EM) structures of the type III-E effector *Sb*-gRAMP-crRNA in complex with TPR-CHAT, with and without target ssRNA at resolutions of 3.0 Å and 2.9 Å, respectively (Supplementary information, Figs. S1, S2 and Table S1). The resulting maps were resolved well enough to facilitate the construction of a de novo model for the gRAMP-crRNA-ssRNA-TPR-CHAT complex (Fig. 1a, b; Supplementary information, Fig. S3). The overall structure of the gRAMP-crRNA-ssRNA-TPR-CHAT complex adopts an "L"-shaped conformation, consisting of a copy of gRAMP, a copy of TPR-CHAT, a 37-nt crRNA, and an 18-nt target ssRNA (Fig. 1b). The length and the width of the gRAMP-crRNA-ssRNA-TPR-CHAT is approximately 145 Å and 96 Å, respectively. The gRAMP is composed of one Cas11 domain and four Cas7 domains. Four Cas7 domains (Cas7.1–Cas7.4) stack along the crRNA on one side, forming a filament (Fig. 1b). The Cas7 domains in gRAMP display RRM folds similar to those observed in type III-A Csm3 and III-B Cmr4, which are composed of a four-stranded antiparallel β-sheet

flanked by three α-helices on one side. A significant difference between the Cas7 domains in gRAMP and Csm3/Cmr4 is that each of the Cas7 domains contains a zinc-finger motif. In the Cas7.1, Cas7.2, and Cas7.4 domains, the zinc ions are coordinated by the C2C2 zinc-finger motif. In contrast, the zinc ion in the Cas7.3 domain is coordinated by the CCCH zinc-finger motif. The Cas11 domain locates on the other side of the crRNA, interacting with Cas7.2, Cas7.3, and target ssRNA (Fig. 1b). Similar to the structures of type III-A Csm2 and III-B Cmr5, the Cas11 domain in gRAMP displays a helix bundle conformation, with three α-helices on one side and two α-helices on the other side (Fig. 1b). The architecture of type III-E effector system is significantly different from those of type III-A and type III-B. The overall structure of the Cmr/Csm complex displays a capsule-like architecture.⁹ Four Cmr4 (three Csm3) and three Cmr5 (two Csm2) subunits constitute the double helical backbone, which is capped by Cmr1–Cmr6 (Csm5) at one end (head) and Cmr2–Cmr3 (Csm1–Csm4) at the other end (tail).

The four Cas7 domains and the single Cas11 domain look like a palm to grasp the crRNA:target ssRNA heteroduplex. The crRNA is composed of a 19-nt 5'-handle and an 18-nt guide segment. The 5'-handle region (G(-19)–C(-1)) lies in the groove formed by the Cas7.1 and Cas7.2 domains (Fig. 1b; Supplementary information, Tables S2 and S3). The crRNA:target ssRNA heteroduplex (C(1):G(-1)–G(16):C(-16)) is enclosed by the Cas7.2, Cas7.3, and Cas11 domains (Fig. 1b). Due to the insertion of thumb-like β-hairpins in the Cas7.2 and Cas7.3 domains, bases in the crRNA:target ssRNA heteroduplex at the 4th and 10th positions flip outside. Furthermore, a loop (residues 1458–1464) in Cas7.4 passes through the heteroduplex, twisting the bases between positions 13 and 14. The interaction between gRAMP and the crRNA:target ssRNA heteroduplex is mediated by extensive hydrogen bonds and hydrophobic contacts (Fig. 1c). As observed in the structure, the C(-16) in the handle region of crRNA forms hydrogen bonds with Lys47 and Lys55 in Cas7.1 (Fig. 1c). In Cas7.1, U(-15) forms π–π stacking and hydrogen bonds with Phe57 and Asp157, respectively. U(-14)–A(-12) makes hydrophobic stacking with Arg64, His143, Tyr149, and His152 in Cas7.1. U(-11)–G(-10) forms hydrogen bonds with Lys141 and Lys101 in Cas7.1. U(-9) forms π–π stacking with Phe104 in Cas7.1. C(-8) and G(-5) form hydrogen bonds with Arg510 (Cas7.2) and Lys107 (Cas7.1), respectively. A(-7) forms cation–π stacking with Arg37, and C(-6) forms cation–π stacking with Lys229 and Arg472. G(-4) forms π–π stacking and hydrogen bond with Phe192 and Arg37 in Cas7.1, respectively. G(-3) forms a hydrogen bond with Arg481 in Cas7.2. The interactions between gRAMP and the crRNA:target ssRNA heteroduplex are mainly mediated by the sugar-phosphate backbone and the neighboring basic amino acids, including His327, His328, Arg294, Arg323, Lys371, Asp698, Arg728, Arg732, Arg1004, Arg1008, Lys1426, Lys1479, Arg1505, and Lys1553

Received: 26 June 2022 Accepted: 7 October 2022
Published online: 24 October 2022

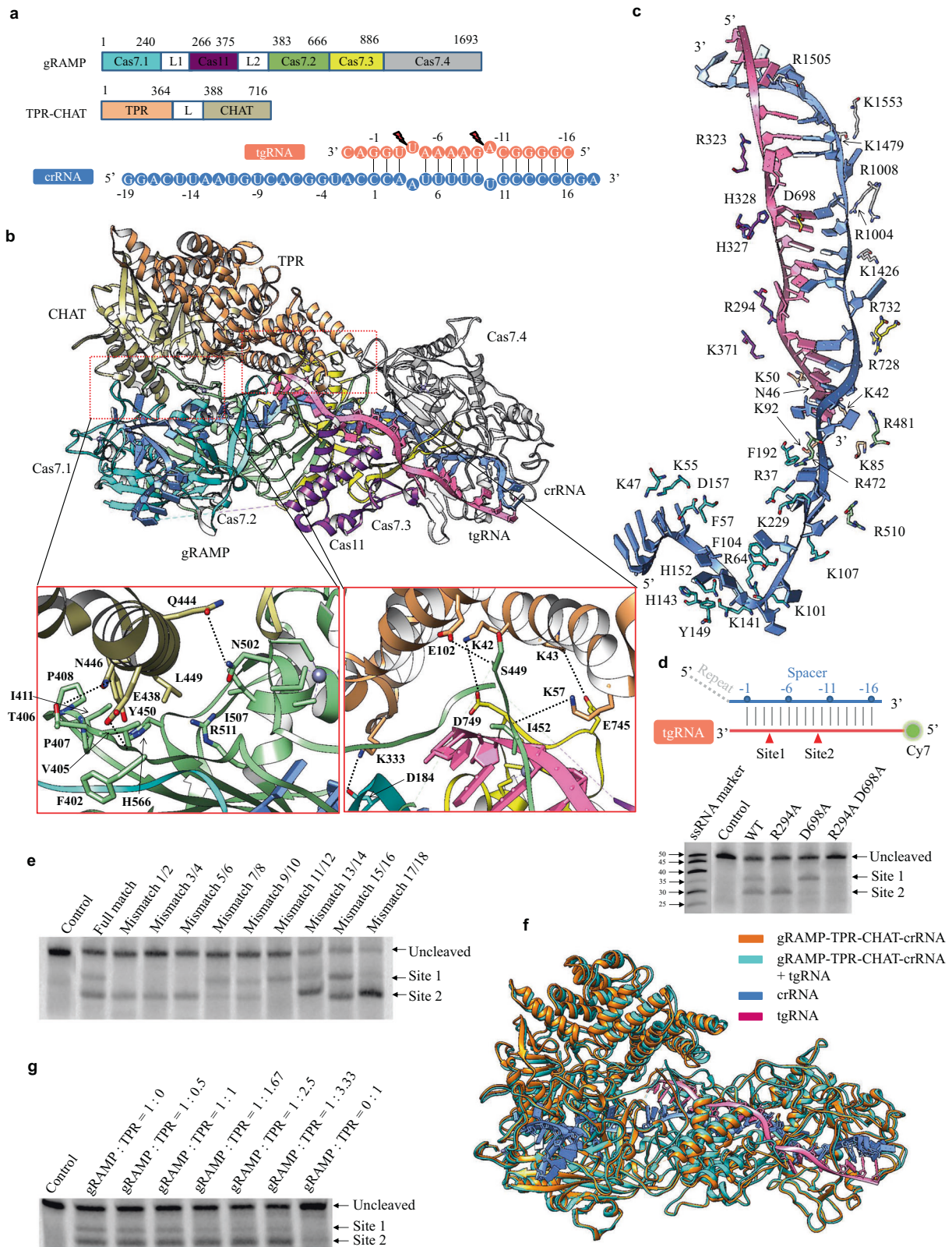


Fig. 1 Cryo-EM structure of the gRAMP in complex with TPR-CHAT. **a** Graphic representation of the domain organization of the gRAMP and TPR-CHAT proteins. Schematic representation of the crRNA:target ssRNA heteroduplex. The target ssRNA cleavage sites are labeled. **b** Illustration of the overall structure of the gRAMP-crRNA-ssRNA-TPR-CHAT complex. The Cas7.1, Cas11, Cas7.2, Cas7.3, Cas7.4, TPR, and CHAT domains are shown in cyan, purple, green, yellow, gray, goldenrod, and sandy brown, respectively. **c** Illustration of the interactions between gRAMP and the bound nucleic acids. Colors used to represent interaction residues are the same as those shown in **b**. **d** Cleavage activity analysis of wild-type (WT) gRAMP and its mutants. **e** In vitro target ssRNA cleavage by the WT gRAMP using mismatched RNAs. **f** Structural comparison of gRAMP-crRNA-TPR-CHAT with or without target ssRNA. The gRAMP-crRNA-TPR-CHAT complex is shown in cyan and gRAMP-crRNA-ssRNA-TPR-CHAT is shown in orange. **g** In vitro target ssRNA cleavage assay of gRAMP in the presence of TPR-CHAT.

(Fig. 1c). A previous study has shown that gRAMP cleaves target ssRNA at two defined positions, which are located after the 3rd and 9th nucleotides, six nucleotides apart.⁷ In the structure of gRAMP–crRNA–ssRNA–TPR-CHAT, residue Arg294 in Cas7.2 neighbors the phosphodiester bonds between the 3rd and 4th nucleotides, whereas residue Asp698 in Cas7.3 neighbors the phosphodiester bonds between nucleotides 9 and 10. To investigate whether the residues Arg294 and Asp698 are responsible for cleaving the target ssRNA, R294A and D698A mutants were constructed (Supplementary information, Table S4). The enzymatic activity assay results showed that the R294A and D698A mutations abolished the ability to cut target ssRNA at one cleavage site, indicating that residues of Arg294 in Cas7.2 and Asp698 in Cas7.3 are vital for ribonuclease activity (Fig. 1d). We further performed *in vitro* target ssRNA cleavage by the gRAMP using mismatched RNAs. As shown in Fig. 1e, mismatches 1/2, 3/4, and 5/6 abolished the target RNA (tgRNA) cleavage at site 1. In contrast, mismatch 11/12 abolished the tgRNA cleavage at site 2. Mismatch 7/8 decreased the tgRNA cleavage at site 2, while mismatch 9/10 decreased the tgRNA cleavage at both site 1 and site 2. Interestingly, the cleavage of mismatched RNAs 13/14, 15/16, and 17/18 was improved (Fig. 1e; Supplementary information, Fig. S4 and Table S5). The data suggested that the base pairings surrounding positions 3 and 9 are vital for the tgRNA cleavage. The gRAMP and crRNA both contribute to the binding of tgRNA. The mismatch between crRNA and tgRNA can seriously weaken the interaction between gRAMP–crRNA and tgRNA. Thus, the product RNA would be more prone to dissociating from the crRNA. The mismatch between crRNA and tgRNA can promote substrate turnover, thus increasing the endoribonuclease activity.

TPR-CHAT is a 716-residue protein that consists of two domains (Fig. 1a). The N-terminal TPR domain displays a 16 α -helix bundle conformation. The C-terminal CHAT domain contains an 11-stranded antiparallel β -sheet flanked by four α -helices on one side and five α -helices on the other side (Fig. 1b). Structural alignment using the DALI server indicates that TPR-CHAT exhibits a peptidase fold. TPR-CHAT is located adjacent to Cas7.1, Cas7.3, and the 3'-end of the target ssRNA (Fig. 1b). The interface between TPR-CHAT and gRAMP–crRNA–ssRNA buries a solvent-accessible surface area of $\sim 1435 \text{ \AA}^2$, and contains extensive hydrogen bonds (involving Lys57, Glu102, Glu438, Asn446, and Gln444 in TPR-CHAT, and Ile452, Ser449, Phe402, Thr406, and Asn502 in gRAMP), salt bridges (involving Lys42, Lys43, and Lys333 in TPR-CHAT, and Asp749, Glu745, and Asp184 in gRAMP), and hydrophobic interactions (involving Leu449 and Tyr450 in TPR-CHAT, and Val405, Pro407, Pro408, Ile411, His566, Ile507, and Arg511 in gRAMP) (Fig. 1b). Notably, TPR-CHAT also makes direct contacts with the target ssRNA (Fig. 1c). Residues Lys42, Lys85, and Lys92 form hydrogen bonds with phosphate moieties of A(–3)–C(–4). Residues Asn46 and Lys50 form hydrogen bonds with phosphate moieties of G(–2)–A(–3) and G(–1)–G(–2), respectively (Fig. 1c).





Structural superimposition of gRAMP–crRNA–TPR-CHAT with or without target ssRNA yields a root mean square deviation (RMSD) of 1.042 \AA over 1909 aligned Ca atoms, indicating that target ssRNA binding does not cause the extensive rearrangement of gRAMP and TPR-CHAT (Fig. 1f). However, it is worth noting that, due to the direct interaction between the N-terminal TPR domain and the 3'-end of target ssRNA, the TPR domain draws slightly closer to the crRNA:target ssRNA heteroduplex (Fig. 1f). TPR-CHAT could enforce the interactions between gRAMP and target ssRNA, which would hinder the dissociation of products from the crRNA and weaken the enzymatic activity. To explore the effect of TPR-CHAT on the target ssRNA cleavage by gRAMP, we performed an *in vitro* target ssRNA cleavage assay by adding increasing molar concentrations of TPR-CHAT. As shown in Fig. 1g, the cleavage activity of gRAMP at site 1 was decreased when the higher

concentrations of TPR-CHAT were included in the reaction. We speculate that this may be caused by the location of site 1, which is closer to TPR-CHAT. A new target ssRNA could bind at site 2 while site 1 is still occupied by the previous product. Thus, the cleavage activity of gRAMP at site 1 is decreased, while the activity at site 2 appears unaffected.

Taken together, these results provide the atomic view of the architecture of Craspase. Combining mutagenesis experiments and structural information enabled the further identification of two catalytic residues in gRAMP for target ssRNA cleavage. The insertion domain (residues 1031–1390) and part of the crRNA (bases 19–38) were not observed in our structure due to the flexibility. We also tried the focused 3D classification and local refinement; however, the density of the insertion domain was still not observed. The mismatched RNAs (mismatches 13/14, 15/16, and 17/18) increase the enzymatic activity, possibly because the mismatched target ssRNAs (13/14, 15/16, and 17/18) are more prone to dissociating from the crRNA. During the preparation of this manuscript, the structure of *Desulfonema ishimotonii* Cas7-11 (*DiCas7-11*) in complex with crRNA and target ssRNA was reported at 2.5 \AA resolution.¹⁰ *Sb*-gRAMP shares 34% sequence identity with *DiCas7-11* (Supplementary information, Fig. S5). Structural comparison of these two structures indicates that the overall structure of *Sb*-gRAMP adopts a similar fold to that of *DiCas7-11*, with both containing one Cas11 domain and four Cas7 domains (Supplementary information, Fig. S6). In addition, the crRNA and target ssRNA also display similar conformations. The RMSD of these two structures is 2.05 \AA for the aligned 848 Ca atoms. The major difference between these two structures is that the Cas11 domain rotates $\sim 30^\circ$, and the insertion domain is not observed in our structure due to flexibility (Supplementary information, Fig. S6). Recently, Nishimasu's group resolved the cryo-EM structures of the *DiCas7-11*–crRNA–Csx29 complex with and without target ssRNA.¹¹ In the structure of *DiCas7-11*–crRNA–Csx29–tgRNA, the CTD of Csx29 (residues 75–751) is not observed. The author proposed that upon the target ssRNA binding, Csx29 adopts a flexible conformation, which allows the active center to access the substrate protein. However, in our structure, the density of TPR-CHAT is clearly observed. Structural superimposition of TPR-CHAT with or without target ssRNA indicates that the helix bundle in the TPR domain moves slightly toward crRNA. In addition, the protease active center is solvent exposed in the target ssRNA to allow the access to the substrate protein (Supplementary information, Fig. S7). We just noticed that Ke's group resolved the structures of Craspase in four different states, including resting state, non-matching PFS RNA bound state, matching PFS RNA bound state, and non-matching PFS RNA post-cleavage state. They found that the binding of target ssRNA with a non-matching PFS would cause a rigid body movement of CHAT domain, which results in the change in distance between catalytic residues C627 and H585 from 6.6 \AA to 3.3 \AA . However, we did not observe dramatic conformational changes in CHAT domain. This may be due to the fact that the length of PFS sequence observed in our structure is 3 bp shorter than that resolved by Ke's group. Previous study supports the possibility that the type III-E CRISPR-Cas system could trigger abortive infection using a caspase-like peptidase, whereby host cells suicide to prevent phages from spreading beyond the infected cell. Nishimasu's group revealed that the caspase-like peptidase TPR-CHAT functions to cleave the type III-E-associated Csx30 and release the toxic N-terminal fragment, which in turn triggers the cell growth arrest or cell death through inhibiting the RpoE activity.¹²

In summary, the data presented in this study reveal the mechanism of recognition of crRNA and target ssRNA by gRAMP. The structures provide insights into pre-crRNA processing and target ssRNA cutting. Furthermore, this work reports the structure of the CRISPR type III-E effector in complex with the binding partner TPR-CHAT, providing vital clues for elucidating

the functional relationship between the CRISPR-Cas system and caspase peptidase.

Shuo Wang ^{1,3}, Minghui Guo ^{1,3}, Yuwei Zhu ^{1,3}
Zhiying Lin¹ and Zhiwei Huang ^{1,2} ✉

¹HIT Center for Life Sciences, School of Life Science and Technology, Harbin Institute of Technology, Harbin, Heilongjiang, China.

²Westlake Center for Genome Editing, Westlake Laboratory of Life Sciences and Biomedicine, School of Life Sciences, Westlake University, Hangzhou, Zhejiang, China. ³These authors contributed equally: Shuo Wang, Minghui Guo, Yuwei Zhu.

✉email: huangzhiwei@hit.edu.cn

DATA AVAILABILITY

The atomic coordinates of the gRAMP–crRNA–TPR-CHAT and gRAMP–crRNA–ssRNA–TPR-CHAT complexes have been deposited to the Protein Data Bank under the accession numbers 7Y8T and 7Y8Y, respectively. The corresponding maps have been deposited in the Electron Microscopy Data Bank under the accession numbers EMD-33685 and EMD-33686, respectively.

REFERENCES

1. Koskella, B. & Brockhurst, M. A. *FEMS Microbiol. Rev.* **38**, 916–931 (2014).
2. Marraffini, L. A. & Sontheimer, E. J. *Nat. Rev. Genet.* **11**, 181–190 (2010).
3. Makarova, K. S. et al. *Nat. Rev. Microbiol.* **18**, 67–83 (2020).
4. Sander, J. D. & Joung, J. K. *Nat. Biotechnol.* **32**, 347–355 (2014).
5. Fagerlund, R. D., Staals, R. H. & Fineran, P. C. *Genome Biol.* **16**, 251 (2015).
6. Cox, D. B. et al. *Science* **358**, 1019–1027 (2017).
7. van Beljouw, S. P. et al. *Science* **373**, 1349–1353 (2021).
8. Özcan, A. et al. *Nature* **597**, 720–725 (2021).
9. Taylor, D. W. et al. *Science* **348**, 581–585 (2015).

10. Kato, K. et al. *Cell* **185**, 2324–2337.e16 (2022).

11. Hu, C. et al. *Science* **377**, 1278–1285 (2022).

12. Kato, K. et al. *bioRxiv* <https://doi.org/10.1101/2022.08.17.504292> (2022).

ACKNOWLEDGEMENTS

We thank Anqi Zhang and Changyou Guo of the EM platform at the School of Life Science and Technology of Harbin Institute of Technology for sample screening and data collection. This research was funded by the National Natural Science Foundation of China (31825008 and 31422014), the Tencent Foundation, and Heilongjiang Touyan Team (HITTY-20190034) to Z.H., and the fellowship of China National Postdoctoral Program for Innovative Talents (BX20200110) to M.G.

AUTHOR CONTRIBUTIONS

S.W., M.G., and Z.L. prepared the samples and performed functional assays. S.W. and M.G. performed negative staining. Y.Z. and Z.H. performed cryo-EM data processing and model building. S.W., Y.Z., and Z.H. wrote the manuscript. Z.H. supervised the study and edited the manuscript.

COMPETING INTERESTS

The authors declare no competing interests.

ADDITIONAL INFORMATION

Supplementary information The online version contains supplementary material available at <https://doi.org/10.1038/s41422-022-00738-3>.

Correspondence and requests for materials should be addressed to Zhiwei Huang.

Reprints and permission information is available at <http://www.nature.com/reprints>